Title	A Novel Iterative Structure for Online Calibration of M-Channel Time-Interleaved ADCs
Author(s)	Tsui, KM; Chan, SC
Citation	IEEE Transactions on Instrumentation and Measurement, 2014, v. 63 n. 2, p. 312-325
Issued Date	2014
URL	http://hdl.handle.net/10722/189088
Rights	IEEE Transactions on Instrumentation and Measurement. Copyright © Institute of Electrical and Electronics Engineers.

A Novel Iterative Structure for Online Calibration of M-Channel Time-Interleaved ADCs

K. M. Tsui and S. C. Chan, *Member, IEEE*

***Abstract*— This paper proposes a computationally efficient calibration structure for online estimation and compensation of offset, gain and frequency response mismatches in M-channel time-interleaved (TI) analog-to-digital converters (ADCs). The basic idea of the proposed approach is to reserve some sampling instants for estimating and tracking the mismatch parameters of sub-ADCs with reference to a known input. Since the estimation problem is analogous to a standard system identification problem, we propose two simple variable digital filter (VDF) based adaptive filter structures which are derived from the least mean squares (LMS) and normalized LMS algorithms. On the other hand, the reservation of some sampling instants in the normal operation of TI ADC implies that part of samples have to be sacrificed. Based on a general time-varying linear system model for the mismatch and the spectral property of a slightly oversampled input signal, we also propose a novel iterative framework to solve the resulting underdetermined problem. It not only embraces a number of iterative algorithms for the tradeoff between convergence rate and arithmetic complexity but also admits efficient update structure based again on VDFs. Therefore, thanks to the well-known efficient implementation of VDFs, the adaptability of both estimation and compensation algorithms allows us to combine them seamlessly to form an online calibration structure, which is able to track and compensate for the channel mismatches with low complexity and high reconstruction accuracy. Finally, we demonstrate the usefulness of the proposed approach by means of computer simulations.**

***Index Terms*— Calibration, estimation, Farrow structure, frequency response mismatch, gain mismatch, iterative compensation, offset mismatch, time-interleaved analog-to-digital converter (TI ADC).**

I. Introduction

THE operating speed of modern electronic systems, such as software radio [1], [2], is getting higher and higher, and hence there is a growing need for digital instruments to record and measure the relevant system parameters with sufficiently high speed. This calls for high-speed analog-to-digital converters (ADCs), which can deliver increasingly high sampling rate. Given the limitation of current device technology and other cost constraints, time-interleaved (TI) ADC has emerged as a promising approach to achieve this desired high sampling rate by parallel operation of multiple sub-ADCs with lower rate [3]. However, any small channel mismatches such as offset, gain, time, bandwidth, or more general frequency response mismatches, between sub-ADCs degrade the performance significantly [4], [5], and therefore they need to be estimated and corrected.

Recently, a number of efficient compensation structures have been proposed to deal with the mismatches. While most earlier works such as [6]–[15] are mainly concerned with timing mismatch, several recent works in [16]–[21] place emphasis on the compensation of frequency response mismatch, which can be viewed as a general representation of timing and bandwidth mismatches. Among these works, the cascade structure in [20] and a similar approach in [19] are especially attractive for real-time applications because of their relatively low reconfigurable complexity. Later, in [21], it was shown that these methods actually share the idea of a classical iterative algorithm called Richardson iteration (RI) for solving system of linear equations. In this regard, a more versatile iterative framework, including other more efficient iterative algorithms such as Gauss–Seidel iteration (GSI), has been proposed in [21]. Although most conventional compensation structures provide an efficient way to compensate for the mismatches, they only presume that the related mismatch parameters are known or precisely estimated from other external estimation modules. In general, the estimation can be carried out in either foreground [22], [23] or background [24], [25] of the system operation. For the former, a known test or training signal is injected into the system, and hence the operation of the TI ADC has to be stopped during estimation. For background estimation, the mismatch parameters can be determined by some prior knowledge of input signals. Since the estimation process depends solely on the TI ADC output, it does not interrupt the normal operation of TI ADC. However, a large number of samples are usually required to fully meet the condition derived from the prior knowledge, and therefore the convergence rate of background estimation is in general slower than that of the foreground estimation with a known reference signal.

Blind calibration techniques, on the other hand, have also received great attention and they aim at simultaneously estimating and compensating for mismatches. During the past decade, numerous approaches have been proposed. Most of them have been devoted to one or at most two types of mismatches at the same time such as gain mismatch in [26], timing mismatch in [27]–[30], bandwidth mismatch in [31], offset and gain mismatches in [32], gain and timing mismatches in [33] and [34], as well as gain and frequency response mismatches in [35].

Similar to blind estimation, prior knowledge of input signal or other extra information is required in the calibration process. For example, a blind calibration approach was developed in [30] under the wide sense stationary input assumption.

Manuscript received December 19, 2012; revised June 10, 2013; accepted June 16, 2013. Date of publication September 16, 2013; date of current version January 2, 2014. The Associate Editor coordinating the review process was Dr. Niclas Bjorsell.

The authors are with the University of Hong Kong, Hong Kong (e-mail: kmtsui@eee.hku.hk; scchan@eee.hku.hk).

Color versions of one or more of the figures in this paper are available online at http://ieeexplore.ieee.org.

Digital Object Identifier 10.1109/TIM.2013.2278574

Another semi-blind calibration approach in [31] assumed that there is no signal content in both low-pass and high-pass regions, and calibrated the system with a known test signal which does not interfere with the input spectrum. A more commonly used additional knowledge is obtained by assuming that the input signal is slightly oversampled, meaning that no signal exists in the high-pass region. The central idea of several conventional approaches has been based on this mild assumption [27]–[29], [33]–[35].

Another important issue of blind calibration is the computational complexity of updating the adaptive parameters. A computationally efficient structure is highly desired to make it truly suitable for real-time operation of TI ADCs. Therefore, most conventional calibration approaches have been accompanied by efficient implementation structures which can usually be realized using fixed digital filters together with few adaption parameters. These include the filter bank structure in [29] and [33], cascade compensation structure in [28], [34], and [35], polyphase structure in [27], and another filtering structure in [30]. In real-time applications, these approaches are preferable over other block-based algorithms whose complexity usually increases exponentially with large and unknown number of samples.

All of the blind calibration approaches mentioned above have their own strengths and limitations. One common drawback is, however, their slow convergence rate, which is similar to the problem encountered in blind estimation. Very often, a considerable number of samples is required in order to get the first corrected sample with sufficient accuracy. Nevertheless, from the above discussion and other common considerations, one can identify several desirable properties that a versatile calibration structure should possess in order to fully exploit the advantages of TI ADCs. In short, it should 1) be capable of simultaneously handling various types of mismatches, 2) work with mild input spectrum assumption, 3) have computationally efficient structure for easy adaptation to any system changes, 4) exhibit fast convergence rate, 5) allow high input bandwidth efficiency, 6) be applicable to arbitrary number of channels, and 7) offer sufficient reconstruction accuracy. Obviously, it is not easy to achieve all these goals.

In this paper, we attempt to develop such a calibration approach and propose a computationally efficient structure to simultaneously correct offset, gain, and frequency response mismatches in M-channel TI ADCs. The basic idea is to reserve some sampling instants for estimating the mismatch parameters of sub-ADCs during the normal operation of TI ADC. For this propose, a known test signal is first injected into the system at these reserved instants to obtain the corresponding sampled sequence from the sub-ADCs at one end. Then, with the known samples of the test input at the other end, the estimation can be performed similar to a typical system identification problem. For efficient implementation, we follow the polynomial model in [19]–[21] to mimic the slightly different frequency responses of sub-ADCs, which should normally share identical frequency characteristics. The major advantage of the polynomial model is that the change of frequency response mismatches can be well characterized by a variable digital filter (VDF) whose response can be adjusted by a single tuning parameter in an efficient Farrow structure [1], [36], [37]. Consequently, together with simple adaptive filters such as the least mean squares (LMS) and normalized LMS (NLMS) algorithms, various mismatch parameters can be adaptively estimated and tracked with low complexity in real time.

Once the estimated mismatch parameters are available, the major remaining problem is to compensate for the frequency response mismatch because the offset and gain mismatches can be directly corrected at the sub-ADCs' outputs. In this paper, we follow the setting of linear system in our efficient iterative framework previously reported in [21], and propose a novel iterative framework to deal with the compensation problem. However, we note that the present problem is considerably complicated by the fact that part of the samples have been purposely discarded for online estimation of the mismatch parameters. This results in an underdetermined system of linear equations, for which the iterative framework in [21] is not directly applicable. Central to our new development to overcome this difficulty is the skillful incorporation of the spectral property of slightly oversampled input signal into the underdetermined system. This not only allows the iterative framework in [21] to be adopted to solve the new problem but also inherits its important advantages of efficient compensation structures. Several major advantages of the new compensation scheme can be summarized as follows: 1) it embraces a number of iterative algorithms, such as RI and GSI, offering different tradeoffs between implementation complexity and convergence rate; 2) it can be implemented efficiently using VDF which allows the recovery of the desired sequence in a sample by sample manner and enables the online adaptation of the possibly changing channel mismatches with low complexity; 3) its implementation complexity is independent of the number of channels and only a few iterations are required for convergence; and 4) the convergence analysis can be conveniently carried out in time–frequency domain for performance prediction. Simulation results show that combining both estimation and iterative compensation structures leads to a very efficient online calibration structure which is able to meet most of the desired properties mentioned earlier.

The rest of this paper is organized as follows. Section II describes the background of the calibration problem with offset, gain, and frequency response mismatches, and summarizes some related system aspects and details studied in [21]. Section III is devoted to the proposed general system architecture, which mainly consists of separate estimation and iterative compensation modules. The details of these two modules are, respectively, discussed in Sections IV and V. Design examples and comparisons with other conventional approaches are presented in Section VI. Finally, conclusion is drawn in Section VII.

II. Background

In an M-channel TI ADC, as shown in Fig. 1, there are M parallel sub-ADCs operating in a TI manner. An aggregate sampling rate of $f_s = 1/T$ can be achieved when the mth sub-ADC samples the input signal $x_c(t)$ at time $t = kMT + mT$

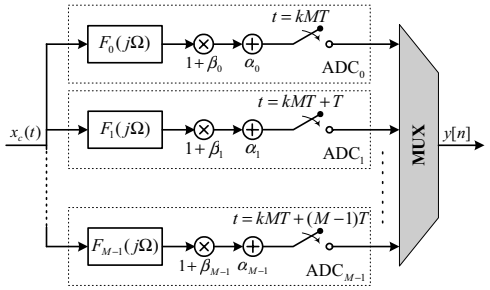

Fig. 1. General structure of an M-channel time-interleaved ADC with various kinds of channel mismatches.

for integer k. However, calibration of the TI ADC is usually required to estimate and compensate for any small mismatches between the M sub-ADCs in order to improve the overall system performance. Typical mismatches are also illustrated in Fig. 1, where the mth sub-ADC exhibits its own offset α_m, gain $(1+\beta_m)$, and frequency response $F_m(j\Omega)$. Because of these mismatches, one can only obtain an uncalibrated output $y[n]$, which deviates considerably from the expected output $x[n] = x_c(nT)$.

Blind calibration is a common approach to jointly estimate and compensate for the mismatches to recover $x[n]$ during the normal operation of TI ADCs. Unfortunately, it always suffers from a long latency to obtain the first valid sample which incurs high complexity and delay for real-time operation. On the other hand, compensation-only structure offers an effective means to perform compensation, but relies on precise knowledge of the mismatches obtained by either foreground or background estimation. In foreground estimation, a known test or training signal is required and hence the operation of TI ADC has to be stopped during estimation. In background estimation, TI ADC can operate as usual. However, like blind calibration, one has to wait for a sufficiently accurate estimate.

In this paper, we propose a novel calibration structure that permits simultaneous estimation and compensation of the mismatches of TI ADC. However, it is interesting to note that the proposed structure does not belong to the category of blind calibration, nor is it a kind of compensation-only structure. Actually, it is more like a compensation-only structure but allows foreground estimation during the normal operation of TI ADCs. We show later that our previously proposed iterative framework in [21], which can be treated as a compensation-only structure, plays an important role in developing the new calibration structure considered in this paper. Because of page limitations, below we only summarize the major results of [21] that are useful to our subsequent discussions. For simplicity, we also ignore the offset and gain mismatches in this section because they can be easily corrected at the sub-ADCs' outputs should they be precisely estimated.

We start with the commonly used band-limiting assumption that the input signal $x_c(t)$ is slightly oversampled by a factor of

$$\frac{1}{\varepsilon} = \frac{f_s}{(2f_{\max})} \tag{1}$$

where $0 < \varepsilon < 1$ is the band-limiting parameter and $f_{\max}$ is the maximum frequency of $x_c(t)$. Therefore, $x_c(t)$ can be exactly recovered from its uniform samples $x[n]$ according to sampling theorem. Hence, the problem of compensating for the frequency response mismatch is equivalent to recovering $x[n]$ from $y[n]$. We first establish an ideal discrete-time (DT) model of TI ADCs with frequency response mismatches as follows:

$$y[n] = \sum_{k=-\infty}^{\infty} x[k] \cdot f_n(n-k) \tag{2}$$

where $f_n(n_0)$ is the DT impulse response of the channel filter $F_n(e^{j\omega}) = F_n(j\Omega)$, and $|\omega| = |\Omega T| \le \pi$ at time instant n. Note that the above linear system may be viewed as an M-periodic time-varying linear system with $F_m(j\Omega) = F_{n \bmod M}(j\Omega)$ or $F_n(j\Omega) = F_{n+M}(j\Omega)$ if M channel filters keep unchanged for a fair amount of time. Intuitively, we can see from (2) that $x[n]$ can be found by de convoluting $y[n]$ with the known time-varying filter $f_n(n_0)$. However, such deconvolution is considerably complicated by the infinite support and time-varying nature of $f_n(n_0)$. Fortunately, from the assumption in (1), we know that the DT Fourier transform (DTFT) of $x[n]$ is zero for $\varepsilon\pi \le |\omega| \le \pi$. Therefore, we can approximate $f_n(n_0)$ by a practical finite-length filter $h_n(n_0)$, say a finite impulse response (FIR) filter, in the frequency band of interest (i.e., $0 \le |\omega| \le \varepsilon\pi$). Hence, (2) can be approximated as

$$y[n] \approx \sum_{k=n-N_{h2}}^{n+N_{h1}} x[k] \cdot h_n[n-k] \qquad \forall n \tag{3}$$

where N_{h1} and N_{h2} are positive integers. We can see that $h_n(n_0)$ has a support of $N_{h1}+N_{h2}+1$ samples with $h_n(0)$ as its center impulse response. For simplicity, we will only focus on the FIR case with finite $N_h = N_{h1} = N_{h2}$. In practice, the differences between the two systems in (2) and (3) can be made arbitrarily small by reducing the approximation error between $f_n(n_0)$ and $h_n(n_0)$. For notation convenience, we shall replace the approximate sign in (3) by the equality sign subsequently.

By assuming that $\{y[n]\}$ and $\{x[n]\}$ are causal sequences with a large number of samples N, we can rewrite (3) in its matrix form as

$$\boldsymbol{y} = \boldsymbol{A}\boldsymbol{x} \tag{4}$$

where $\boldsymbol{y} = [y[0], \ldots, y[N-1]]^T$, $\boldsymbol{x} = [x[0], \ldots, x[N-1]]^T$ and $[\boldsymbol{A}]_{n,k} = h_n[n-k]$, $n, k = 0, 1, \ldots, N-1$. For the sake of presentation, $h_n(n_0)$ is assumed to be noncausal, which can be made causal easily in practical implementation. Since N is usually large but unknown in real-time applications, e.g., TI ADC systems, directly computing the inverse of $\boldsymbol{A}$ is not recommended. In [21], we have proposed to solve (4) using the following iteration:

$$\boldsymbol{B}\boldsymbol{x}^{(m+1)} = \boldsymbol{C}\boldsymbol{x}^{(m)} + \boldsymbol{y} \tag{5}$$

where $\boldsymbol{B} - \boldsymbol{C} = \boldsymbol{A}$, $\boldsymbol{x}^{(m)}$ denotes the solution in the ith iteration, and the initial guess is set as $\boldsymbol{x}^{(0)} = \boldsymbol{y}$. Equation (5) represents a general framework that includes a number of

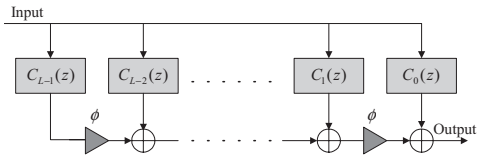

Fig. 2. Farrow structure for implementing a VDF.

iterative methods such as RI and GSI. These iterative methods can be, respectively, expressed as

$$\text{RI}: \boldsymbol{x}^{(m+1)} = (\boldsymbol{I} - \boldsymbol{A})\boldsymbol{x}^{(m)} + \boldsymbol{y} \tag{6}$$

$$\text{GSI}: \boldsymbol{x}^{(m+1)} = (\boldsymbol{D} - \boldsymbol{L})^{-1}\boldsymbol{U}\boldsymbol{x}^{(m)} + (\boldsymbol{D} - \boldsymbol{L})^{-1}\boldsymbol{y} \tag{7}$$

where $\boldsymbol{D}$, $\boldsymbol{L}$, and $\boldsymbol{U}$ are, respectively, the diagonal and the negatives of the strictly lower and upper triangular parts of the matrix $\boldsymbol{A}$. One of the advantages of this framework is that the iteration can be implemented in a sample-by-sample manner. For example, the time-domain representation of GSI is

$$x^{(m+1)}[n] = h_n^{-1}[0]\left(y[n] - \sum_{k=n-N_{h2}}^{n-1} x^{(m+1)}[k]\cdot h_n[n-k] - \sum_{k=n+1}^{n+N_{h1}} x^{(m)}[k]\cdot h_n[n-k]\right), \quad n = 0, \ldots, N-1. \tag{8}$$

We can see that causal implementation of this equation is viable because only the past samples of $x^{(m+1)}[n]$ are involved in the second summation term.

For efficient implementation, the two summation terms can be implemented using VDFs, as suggested in [21]. It is based on the principle that all the channel filters of a practical TI ADC should share similar frequency characteristics, but may differ slightly, say, due to component variations in analog circuits. To be specific, the impulse response of such a VDF is given by

$$h_n[n_0] = h[n_0, \phi]|_{\phi=\phi_n} = \sum_{l=0}^{L-1} c_l[n_0]\cdot\phi^l\Big|_{\phi=\phi_n} \tag{9}$$

where $h[n_0, \phi]$ is the impulse response of the VDF under consideration, L is the number of sub filters, $c_l[n_0]$ is the impulse response of the lth subfilter with fixed coefficients, and ϕ is the spectral parameter which can be adjusted online to vary the desired characteristics of the VDF. In (9), ϕ_n is the value of ϕ at time instant n, and the resultant impulse response is therefore related by $h_n(n_0) = h[n_0, \phi_n]$. Another important advantage of (9) is that it can be implemented efficiently using the well-known Farrow structure [1], [36], [37]. This is shown in Fig. 2, where $C_l(z)$ denotes the frequency response of $c_l[n_0]$ for $l = 0, 1, \ldots, L-1$. For the efficient implementation of the GSI in (8), the impulse response of the VDF in (9) is split into two portions for the computation of the two summation terms, each of which can also be implemented using the Farrow structure. For more details, interested readers are referred to [21]. In Section IV, we will also illustrate in detail how to approximate the ideal channel response $f_n(n_0)$ in (2) by the VDF $h[n_0, \phi]$ in (9).

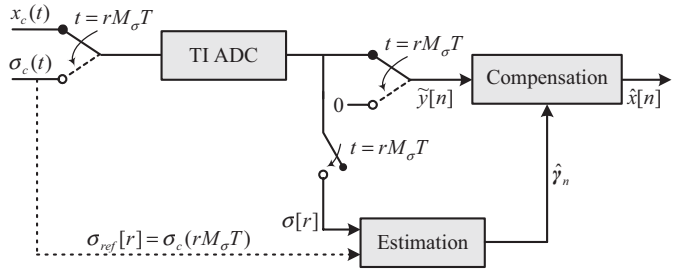

Fig. 3. Structure of the proposed TI ADC system.

Finally, we note from Fig. 2 that the Farrow structure consists of digital subfilters with fixed coefficients and a limited number of variable multipliers for the implementation of the tuning parameter ϕ. As the coefficients of the subfilters are fixed, they can be realized efficiently using sum-of-power-of-two (SOPOT) coefficients instead of expensive general-purpose multipliers [1]. More precisely, these fixed multipliers can be replaced by a limited number of adders and hardwired shifters. Also, if the subfilters are implemented in their transposed form, the redundancy in realizing these SOPOT coefficients can be further reduced by means of multiplier-block technique [38]. Therefore, the resulting iterative structure is amenable to high-speed TI ADCs.

III. Proposed TIADC Structure

In this paper, we consider a new TIADC system shown in Fig. 3, which is able to simultaneously estimate and compensate for the mismatches at an overall sampling rate of $f_s = 1/T$. Apart from a typical TI ADC module as depicted in Fig. 1, it consists of two other main modules, namely estimation and compensation modules. We can see that the proposed system samples the continuous-time (CT) signal $x_c(t)$ at a rate of $f_s = 1/T$ as usual, except that the input is switched to a known signal $\sigma_c(t)$ at time $t = rM_\sigma T$ for integer r. During these particular time instants, the signal $\sigma_c(t)$ [instead of $x_c(t)$] is sampled by one of the sub-ADCs in the TIADC module, and the corresponding DT samples $\sigma[r]$ are collected and then fed into the estimation module. With a known DT sample $\sigma_{\text{ref}}[r] = \sigma_c(rM_\sigma T)$ as another input, the estimation module compares $\sigma[r]$ and $\sigma_{\text{ref}}[r]$ so as to determine the mismatch parameters $\hat{\boldsymbol{\gamma}}_n$ required in the iterative compensation module. These parameters may include offset, gain, and frequency response mismatch parameters of the sub-ADCs discussed in Section II.

Returning to the output of the typical TIADC module, we know from the above mechanism that the samples collected at time $t = rM_\sigma T$ is completely irrelevant to $x_c(t)$, and they have to be discarded before passing them to the compensation module. For the reason which will become apparent later, these samples are replaced by zero via another switch placed after the output of the TIADC module. Consequently, we obtain the following sampled sequence:

$$\tilde{y}[n] = \begin{cases} 0, & n = rM_\sigma \\ y[n], & \text{otherwise.} \end{cases} \tag{10}$$

In the compensation module, $\tilde{y}[n]$ will be used to find $\hat{x}[n]$, which should be close to the desired sequence $x[n] = x_c(nT)$.

Consequently, we need to deal with the following two problems.

1) Estimation of the mismatch parameter $\hat{\boldsymbol{\gamma}}_n$ encapsulated in $\sigma[r]$ with reference to the known sequence $\sigma_{\text{ref}}[r]$.
2) Recovery of $x[n]$ by compensating for the mismatch errors in $\tilde{y}[n]$ with the parameter estimate $\hat{\boldsymbol{\gamma}}_n$.

As mentioned in Section I, the main objective of this paper is to offer satisfactory solutions to the above two problems and develop computationally efficient structures for high-speed and real-time implementation of such TI ADC systems. Below is a brief summary of the major considerations and difficulties of these two problems.

The first problem is similar to a typical system identification problem where $\sigma_c(t)$ can be viewed as a known excitation to the target ADC while its samples $\sigma[r]$ act as a desired sequence measuring the ADC output response. On the other hand, since $\sigma_{\text{ref}}[r]$ is just a known sampled sequence of $\sigma_c(t)$, it can be fed into an equivalent DT model that mimics the response of the target TIADC. The output so obtained can then be compared with $\sigma[r]$ to estimate the set of parameters (i.e., $\hat{\boldsymbol{\gamma}}_n$) that characterizes the model of all sub-ADCs. More details will be discussed in Section IV.

However, the second problem is relatively more difficult because we need to solve an underdetermined system where partial samples of the TI ADC output are deliberately sacrificed in favor of the estimation module. This can be seen from (4) when the number of samples in $\boldsymbol{y}$ is less than N due to the lost samples. Hence, how to guarantee the uniqueness of $\boldsymbol{x}$ and how to solve this problem efficiently would be two of our primary concerns and contributions. In Section V, we will present a computationally efficient iterative framework that greatly extends our previous work in [21] in order to solve simultaneously the frequency response compensation as well as the missing sample problems.

IV. Estimation Module

With the availability of the known input sequence $\sigma_{\text{ref}}[r]$ and the desired sequence $\sigma[r]$, estimating the characteristics of all sub-ADCs is analogous to a system identification problem as mentioned in Section III. Therefore, adaptive filtering algorithms can be utilized to achieve this propose. Before proceeding, we shall examine the choice of M_σ in order to ensure that the proposed adaptive filter has a regular update structure. To this end,we propose to choose M_σ such that

$$M \text{ and } M_\sigma \text{ are coprime.} \tag{11}$$

By so doing, $\sigma[r]$ contains the samples coming from all sub-ADCs. Otherwise, it may happen that only samples of either even-indexed or odd-indexed sub-ADCs are collected. More importantly, the sampling pattern is now repeated for every $M' = MM_\sigma$ samples with respect to $\tilde{y}[n]$ or M samples with respect to $\sigma[r]$. To be specific, within one period, there are M samples in $\sigma[r]$, and each sample is obtained from the kth sub-ADC, where $k = \text{mod}(rM_\sigma, M)$. Owing to the periodicity of k, we can further partition $\sigma[r]$ in M subsampled sequences, each of which corresponds to the samples obtained from only one of the sub-ADCs. For the sake of presentation, we denote such subsampled sequence for the kth sub-ADC by $\sigma_k[r']$, and similarly the corresponding subsampled reference sequence by $\sigma_{\text{ref},k}[r']$. As a result, we can separately estimate the mismatch parameters of the sub-ADCs by considering only their respective subsampled sequences. Moreover, we note that both $\sigma_k[r']$ and $\sigma_{\text{ref},k}[r']$ can be viewed as an M'-fold decimated version of $\sigma_c(nT)$. Hence, to completely avoid aliasing in $\sigma_k[r']$ and $\sigma_{\text{ref},k}[r']$ due to down sampling, we further require that the known signal $\sigma_c(t)$ is band-limited to $f_s/(2M')$ or less. Upon satisfying this mild condition, $\sigma_c(t)$ can be any kind of signals.

Now, we are ready to present the adaptive filtering algorithm in the estimation module. In order to demonstrate the flexibility of the proposed algorithm, we will simultaneously estimate gain, offset, and frequency response of each sub-ADC, which are typical mismatches frequently encountered in TIADCs. To start with, consider the following DT model of the kth sub-ADC

$$\begin{aligned}\hat{\sigma}_k[r', \hat{\boldsymbol{\gamma}}_k] &= \hat{\alpha}_k + (1+\hat{\beta}_k)\cdot\{\sigma_{\text{ref},k}[r'] * h[r', \hat{\phi}_k]\} \\ &= \hat{\alpha}_k + (1+\hat{\beta}_k)\cdot\sum_{l=0}^{L-1}\{\sigma_{\text{ref},k}[r'] * c_l[r']\}\cdot\hat{\phi}_k^l \\ &= \hat{\alpha}_k + (1+\hat{\beta}_k)\cdot\sum_{l=0}^{L-1} u_{k,l}[r']\cdot\hat{\phi}_k^l \end{aligned} \tag{12}$$

where $\hat{\boldsymbol{\gamma}}_k = [\hat{\alpha}_k, \hat{\beta}_k, \hat{\phi}_k]^T$, $*$ denotes the convolution, $u_{k,l}[r']$ is the lth subfilter output, and $\hat{\alpha}_k$, $\hat{\beta}_k$, and $h[r', \hat{\phi}_k]$ are, respectively, its offset, gain, and impulse response. In particular, we note that the frequency response of the kth sub-ADC is represented by its impulse response $h[r', \hat{\phi}_k]$ as in (3), and it follows the VDF model in (9), which is an (L–1) order polynomial function of a single tuning parameter $\hat{\phi}_k$, i.e., $h[r', \hat{\phi}_k] = \sum_{l=0}^{L-1} c_l[r']\cdot\hat{\phi}_k^l$. Then, we can adaptively estimate the parameters $\hat{\boldsymbol{\gamma}}_k$ by minimizing the error between $\sigma_k[r']$ and $\hat{\sigma}_k[r', \hat{\boldsymbol{\gamma}}_k]$ in (12).

In this paper, we will employ the well-known LMS and NLMS algorithms to estimate $\hat{\boldsymbol{\gamma}}_k$ because of their low complexity [39]. Other efficient adaptive filter algorithms may also be used, but we only focus on these LMS-based algorithms for simplicity. First of all, define an error sequence for the kth sub-ADC as

$$e\left[r', \hat{\boldsymbol{\gamma}}_k\right] = \sigma_k\left[r'\right] - \hat{\sigma}_k\left[r', \hat{\boldsymbol{\gamma}}_k\right]. \tag{13}$$

Now consider the objective function

$$C(\hat{\boldsymbol{\gamma}}_k) = 0.5\cdot E\left\{e^2\left[r', \hat{\boldsymbol{\gamma}}_k\right]\right\} \tag{14}$$

where $E\{\bullet\}$ denotes the expectation. The solution of minimizing $C(\hat{\boldsymbol{\gamma}}_k)$ may be determined iteratively via the steepest descent method [39] as

$$\begin{aligned}\hat{\boldsymbol{\gamma}}_k\left[r'+1\right] &= \hat{\boldsymbol{\gamma}}_k\left[r'\right] - \mu\nabla C\left(\hat{\boldsymbol{\gamma}}_k\left[r'\right]\right) = \hat{\boldsymbol{\gamma}}_k\left[r'\right] \\ &\quad -\mu E\left\{e\left[r', \hat{\boldsymbol{\gamma}}_k\left[r'\right]\right]\cdot\nabla e\left[r', \hat{\boldsymbol{\gamma}}_k\left[r'\right]\right]\right\}\end{aligned} \tag{15}$$

where μ is the step size of update, and $\nabla C(\hat{\boldsymbol{\gamma}}_k[r']) = E\{e[r', \hat{\boldsymbol{\gamma}}_k[r']]\cdot\nabla e[r', \hat{\boldsymbol{\gamma}}_k[r']]\}$ denotes the gradient vector

with

$$\nabla e\left[r', \hat{\boldsymbol{\gamma}}_k\right] = \left[\frac{\partial e\left[r', \hat{\boldsymbol{\gamma}}_k\right]}{\partial \hat{\alpha}_k}, \frac{\partial e\left[r', \hat{\boldsymbol{\gamma}}_k\right]}{\partial \hat{\beta}_k}, \frac{\partial e\left[r', \hat{\boldsymbol{\gamma}}_k\right]}{\partial \hat{\phi}_k}\right]^T = \left[1, \sum_{l=0}^{L-1} u_{k,l}\left[r'\right]\hat{\phi}_k^l, (1+\hat{\beta}_k)\sum_{l=1}^{L-1} l u_{k,l}\left[r'\right]\hat{\phi}_k^{l-1}\right]^T. \quad (16)$$

As is common practice, the expectation value in (15) is approximated by its instantaneous value, and hence its update equation can be derived as

$$\hat{\boldsymbol{\gamma}}_k\left[r'+1\right] = \hat{\boldsymbol{\gamma}}_k\left[r'\right] - \mu e\left[r', \hat{\boldsymbol{\gamma}}_k\left[r'\right]\right] \cdot \nabla e\left[r', \hat{\boldsymbol{\gamma}}_k\left[r'\right]\right] \quad (17)$$

which is similar to an LMS algorithm.

Alternatively, one may also employ the Newton's method to compute the argument for minimizing $C(\hat{\boldsymbol{\gamma}}_k)$ [39]

$$\hat{\boldsymbol{\gamma}}_k\left[r'+1\right] = \hat{\boldsymbol{\gamma}}_k\left[r'\right] - \mu\left\{\nabla^2 C\left(\hat{\boldsymbol{\gamma}}_k\left[r'\right]\right)\right\}^{-1} \nabla C\left(\hat{\boldsymbol{\gamma}}_k[r']\right) \quad (18)$$

where $\nabla^2 C(\hat{\boldsymbol{\gamma}}_k[r'])$ denotes the Hessian matrix. To avoid the expensive computation of $\{\nabla^2 C(\hat{\boldsymbol{\gamma}}_k[r'])\}^{-1}$, one can approximate the Hessian matrix as

$$\nabla^2 C\left(\hat{\boldsymbol{\gamma}}_k\left[r'\right]\right) \approx \zeta \boldsymbol{I} + \nabla e\left[r', \hat{\boldsymbol{\gamma}}_k\left[r'\right]\right] \nabla^T e[r', \hat{\boldsymbol{\gamma}}_k\left[r'\right]] \quad (19)$$

where ζ is a small positive regularization parameter as in the Levenberg–Marquart (LM) algorithm, and the product of the Jacobian matrix and its transpose in the Gauss–Newton (GN) method is approximated by the instantaneous gradient. Accordingly, the matrix inversion lemma can be invoked to obtain

$$\{\zeta \boldsymbol{I} + \nabla e\left[r', \hat{\boldsymbol{\gamma}}_k\left[r'\right]\right] \nabla^T e\left[r', \hat{\boldsymbol{\gamma}}_k\left[r'\right]\right]\}^{-1} \cdot \nabla e\left[r', \hat{\boldsymbol{\gamma}}_k\left[r'\right]\right] = \frac{\nabla e\left[r', \hat{\boldsymbol{\gamma}}_k\left[r'\right]\right]}{\zeta + \left\|\nabla e[r', \hat{\boldsymbol{\gamma}}_k\left[r'\right]\right\|^2} \quad (20)$$

from which (18) can be further simplified to

$$\hat{\boldsymbol{\gamma}}_k\left[r'+1\right] = \hat{\boldsymbol{\gamma}}_k\left[r'\right] - \mu \frac{e\left[r', \hat{\boldsymbol{\gamma}}_k\left[r'\right]\right] \cdot \nabla e\left[r', \hat{\boldsymbol{\gamma}}_k\left[r'\right]\right]}{\zeta + \left\|\nabla e[r', \hat{\boldsymbol{\gamma}}_k\left[r'\right]\right\|^2} \quad (21)$$

which can be viewed as an NLMS algorithm. One can similarly derive the corresponding LM or GN algorithms if a window of samples is used instead of the instantaneous value. Since the actual value of $\hat{\boldsymbol{\gamma}}_k$ is usually small in practical TI ADC systems, its initial guess can be simply set to zero. However, there are two important issues regarding the selection of the step size. First, the step size μ can be set smaller to trade a higher accuracy with a slower convergence, or vice versa. Second, while the step size of the LMS update equation in (17) somehow depends on the signal power of $\sigma_c(t)$, a simple choice of $\mu = 1$ in the NLMS algorithm in (21) usually leads to satisfactory convergence performance thanks to the normalization term of $\left\|\nabla e[r', \hat{\boldsymbol{\gamma}}_k[r']\right\|^2$. Therefore, in practical implementation, the NLMS algorithm is preferred over the LMS algorithm in spite of its slightly higher complexity due to the computation of the normalization term.

Moreover, we can see that the calculation of both update equations of LMS and NLMS algorithms mainly hinges on the computation of $\hat{\sigma}_k[r', \hat{\boldsymbol{\gamma}}_k]$ in (12) and the gradient vector $\nabla e[r', \hat{\boldsymbol{\gamma}}_k[r']]$ in (16), which also follow the VDF model in (9). Therefore, they can be implemented efficiently using the Farrow structure as depicted in Fig. 2, and a possible structure of the proposed estimate module is shown in Fig. 4.

V. Iterative Compensation Module

A. Problem Description

Once the estimation module obtains an estimate of $\boldsymbol{\gamma}_n$, one can compensate for the mismatches of TI ADCs. Since offset and gain mismatches can be simply removed at the sub-ADCs' outputs according to $(\tilde{y}[n] - \hat{\alpha}_n)/(1 + \hat{\beta}_n)$ for $n \neq rM_\sigma$, we shall only focus on the compensation of frequency response mismatch. As discussed in Section III, the remaining problem we will encounter is actually a joint TIADC frequency response mismatch problem and missing sample problem, which can be expressed as

$$\boldsymbol{y}_S = S(\boldsymbol{y}) = S(\boldsymbol{A})\boldsymbol{x} = \boldsymbol{A}_S\boldsymbol{x} \quad (22)$$

where $S(\bullet)$ denotes the selection operator that only retains the rows of vector or matrix inside the bracket corresponding to the observed samples at time instants $n \neq rM_\sigma$. Therefore, (22) is an underdetermined system where the exact recovery of $\boldsymbol{x}$ may be infeasible if M_σ is not properly chosen. Fortunately, according to the Nyquist–Landau density or nonuniform sampling theorem [40], a CT input signal can still be uniquely recovered from a set of its nonuniform samples if the average sampling rate is greater than two times the maximum input frequency. In the context of this paper, the common assumption that the target CT signal $x_c(t)$ is slightly oversampled by a factor of $1/\varepsilon$ in (1) offers us sufficient margin to exactly recover $\boldsymbol{x}$ even if part of the samples in $\boldsymbol{y}$ have been discarded. More precisely, if the sampling rate f_s and the maximum input frequency are related by (1), the system is affordable to lose at most $(1-\varepsilon)\times 100\%$ of the samples in $\boldsymbol{y}$. Hence, besides the suggestion in (11) from the point of view of regular adaptive filter update structure, M_σ has to satisfy

$$M_\sigma > 1/(1-\varepsilon) \quad (23)$$

so that only one sample of $x_c(t)$ is actually lost for every M_σ samples. Hence, the average sampling rate can be calculated as $f_a = (M_\sigma - 1)f_s/M_\sigma > \varepsilon f_s = 2f_{\max}$, which meets the condition of the nonuniform sampling theorem.

Although the above choice of M_σ guarantees the recovery of $\boldsymbol{x}$ from $\boldsymbol{y}_S$, we still have to look for any possible additional information on $\boldsymbol{x}$ in order to compensate for the missing information due to the lost samples. One possible way to do so is to make use again of the oversampling assumption in (1), which implicitly implies zero DTFT of $x[n]$ for $\varepsilon\pi \leq |\omega| \leq \pi$, $0 < \varepsilon < 1$. This may also be interpreted as the time-domain relation

$$x[n] = \sum_{k=n-N_w}^{n+N_w} x[k] \cdot w[n-k] \quad (24)$$

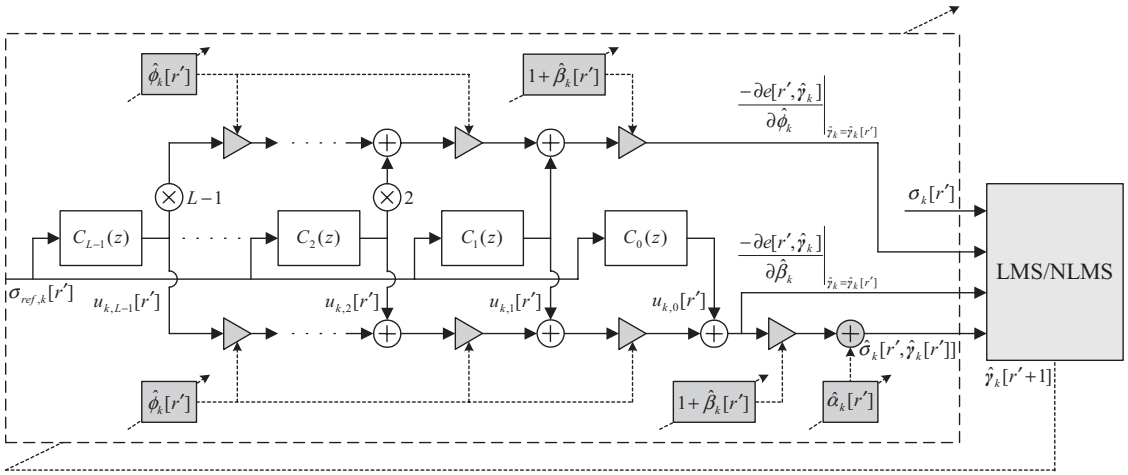

Fig. 4. VDF-based structure of the proposed estimation module.

where $w[n_0]$ is an impulse response of the low-pass filter. For simplicity, we assume that it is a type I linear-phase FIR filter with a passband cutoff frequency at $\omega = \varepsilon\pi$ and a filter length of $2N_w + 1$. Again, we further assume $w[n_0]$ is a zero-phase filter for the ease of presentation. Similar to the definition in (4), (24) can be expressed in matrix form as

$$\boldsymbol{W}\boldsymbol{x} = \boldsymbol{x} \tag{25}$$

where the rows of $\boldsymbol{W}$ are related to $w[n_0]$. This additional information will be the key to restore a square system matrix for which iterative methods naturally work with.

B. Conventional Iterative Frameworks

In this subsection, we briefly review several conventional iterative methods for solving missing sample problem, which employed the prior knowledge in (25) to overcome the system deficiencies. These include the Papoulis–Gerchberg algorithm [41]–[44], Youla's alternating projection algorithm [45], and the constrained iterative restoration algorithm [46]. Although these works were reported independently by different authors, it was suggested in [44] that the resulting algorithm actually belongs to the same form of iteration as

$$\boldsymbol{x}^{(m+1)} = (\boldsymbol{I} - \boldsymbol{D}\boldsymbol{A})\boldsymbol{W}\boldsymbol{x}^{(m)} + \boldsymbol{y} \tag{26}$$

or its alternate form as

$$\boldsymbol{x}^{(m+1)} = \boldsymbol{W}(\boldsymbol{I} - \boldsymbol{D}\boldsymbol{A})\boldsymbol{x}^{(m)} + \boldsymbol{W}\boldsymbol{y} \tag{27}$$

where $\boldsymbol{D}$ is a diagonal matrix with $[\boldsymbol{D}]_{n,n} = 0$ for $n = rM_\sigma$ or $[\boldsymbol{D}]_{n,n} = 1$ otherwise. In this paper, we refer the iterations in (26) and (27) to as constrained iterative algorithm (CIA). Here, we note that the iteration framework in [44] is modified to deal with the frequency response mismatch considered in this paper. When $\boldsymbol{A} = \boldsymbol{I}$, (26) and (27) reduce to the conventional framework of CIA, since the original problem in [44] was only concerned with uniform samples remaining on the regular sampling grid. From the implementation point of view, the CIA can be realized efficiently as a cascade of two digital filters associated with $\boldsymbol{A}$ and $\boldsymbol{W}$, which is similar to the idea we previously reported in [21]. However, when further examining the CIAs in (26) and (27), one can easily notice that both of them indeed belong to the general form of RI in (6) because the system matrices they encounter can be, respectively, viewed as $\boldsymbol{I} - (\boldsymbol{I} - \boldsymbol{D}\boldsymbol{A})\boldsymbol{W}$ and $\boldsymbol{I} - \boldsymbol{W}(\boldsymbol{I} - \boldsymbol{D}\boldsymbol{A})$. As we will illustrate in Section VI, the RI and its related algorithms such as CIA are very ineffective in solving the present problem, and they are usually outperformed by the GSI-based algorithms [21] in terms of the convergence rate. For finite-dimensional problem, the system matrices of the CIAs may alternatively be split as suggested in (7) to form the GSI-based CIA for achieving possible faster convergence. However, in real-time applications such as TI ADCs, the problem dimension is usually unknown, and, therefore, if efficient implementation structure is of interest, the GSI may not be directly applicable in this case because of the coupling of $\boldsymbol{A}$ and $\boldsymbol{W}$. Fortunately, we are able to show later in Section V-C that the GSI under the proposed iterative framework can also be efficiently implemented using the VDF based on Farrow's structure.

There have been other attempts in [47] and [48] to combine (22) and (25) by considering the following regularized least squares problem:

$$\min_{\boldsymbol{x}} \left\| \boldsymbol{y}_S - \boldsymbol{A}_S\boldsymbol{x} \right\|^2 + \lambda \left\| \boldsymbol{W}\boldsymbol{x} - \boldsymbol{x} \right\|^2 \tag{28}$$

where λ is the regularization parameter. Based on its normal equation, the iteration for solving (28) can be written as

$$\boldsymbol{x}^{(m+1)} = (\boldsymbol{I} - \boldsymbol{A}_S^T\boldsymbol{A}_S - \lambda\boldsymbol{W}^T\boldsymbol{W})\boldsymbol{x}^{(m)} + \boldsymbol{A}_S^T\boldsymbol{y}_S \tag{29}$$

which is called regularized iterative algorithm (RIA). Again, we can see that (29) belongs to an RI and the application of GSI may not be so straightforward unless efficient filtering structure is not a concern.

C. Proposed Iterative Framework

In this paper, we take a different way to incorporate (25) into the problem, which facilitates the development of a more efficient and flexible iterative framework than other conventional iterative algorithms mentioned earlier. To start with, we

consider a high-pass filter $\bar{w}[n_0]$, which is complementary to $w[n_0]$ as follows:

$$\bar{w}[0] = 1 - w[0] \text{ and } \bar{w}[n_0] = -w[n_0] \text{ for } n_0 \neq 0. \quad (30)$$

It is clear from (24) that the output of filtering $x[n]$ by $\bar{w}[n_0]$ is simply equal to zero. That is

$$0 = \sum_{k=n-N_w}^{n+N_w} x[k] \cdot \bar{w}[n-k] \quad (31)$$

which can be viewed as an extra information of $x[n]$ regardless of the original time varying system in (3). Similar to (25), we express (31) as

$$\bar{\boldsymbol{W}} x = (\boldsymbol{I} - \boldsymbol{W})\boldsymbol{x} = \boldsymbol{0} \quad (32)$$

where the rows of $\bar{\boldsymbol{W}}$ are constructed from $\bar{w}[n_0]$. Unlike the conventional iterative methods that rely on (25), we are more interested in (32) because it can be used to directly replace the missing sample locations at $n = rM_\sigma$ due to (10). More precisely, it can be incorporated in (22) to form a new system of linear equations as follows:

$$\tilde{\boldsymbol{y}} = \tilde{\boldsymbol{A}} x \quad (33)$$

where $[\tilde{\boldsymbol{y}}]_n = \tilde{y}[n]$ defined in (10) and

$$[\tilde{\boldsymbol{A}}]_n = \begin{cases} [\bar{\boldsymbol{W}}]_n, & n = rM_\sigma \\ [\boldsymbol{A}]_n, & \text{otherwise.} \end{cases} \quad (34)$$

Here, $[\bullet]_n$ denotes the nth entry of vector or row of matrix inside the bracket. This also justifies the insertion of zeros to fill the void of $y[n]$, as suggested in Section III. With the new system (square) matrix $\tilde{\boldsymbol{A}}$ in (33), iterative methods such as RI and GSI introduced in Section II can be applied to solve the missing sample problem in (22). From (5), one can immediately write the new iterative framework as

$$\boldsymbol{x}^{(m+1)} = \tilde{\boldsymbol{G}} \boldsymbol{x}^{(m)} + \tilde{\boldsymbol{B}}^{-1} \boldsymbol{y} \quad (35)$$

where $\tilde{\boldsymbol{G}} = \tilde{\boldsymbol{B}}^{-1}\tilde{\boldsymbol{C}}$, $\tilde{\boldsymbol{B}} - \tilde{\boldsymbol{C}} = \tilde{\boldsymbol{A}}$ and $\boldsymbol{x}^{(0)} = \boldsymbol{y}$.

The major advantage of (35) is that it can be implemented efficiently using Farrow structure as in [21]. Taking the GSI as an example, we obtain from (8) that

$$x^{(m+1)}[n] = \tilde{h}_n^{-1}[0] \left(y[n] - \sum_{k=n-N_{h2}}^{n-1} x^{(m+1)}[k] \cdot \tilde{h}_n[n-k] - \sum_{k=n+1}^{n+N_{h1}} x^{(m)}[k] \cdot \tilde{h}_n[n-k] \right), \quad n = 0, \ldots, N-1 \quad (36)$$

where

$$\tilde{h}_n[n_0] = \begin{cases} \bar{w}[n_0], & n = rM_\sigma \\ h_n[n_0], & \text{otherwise.} \end{cases} \quad (37)$$

Together with the selection criterion of M_σ in (11), we further notice that (37) can be viewed as an M'-periodic time-varying linear system with $M' = MM_\sigma$. Now we rewrite (36) as

$$x^{(m+1)}[n] = \tilde{h}_n^{-1}[0] \left(y[n] - s_1^{(m)}[n] - s_2^{(m)}[n] \right) \quad (38)$$

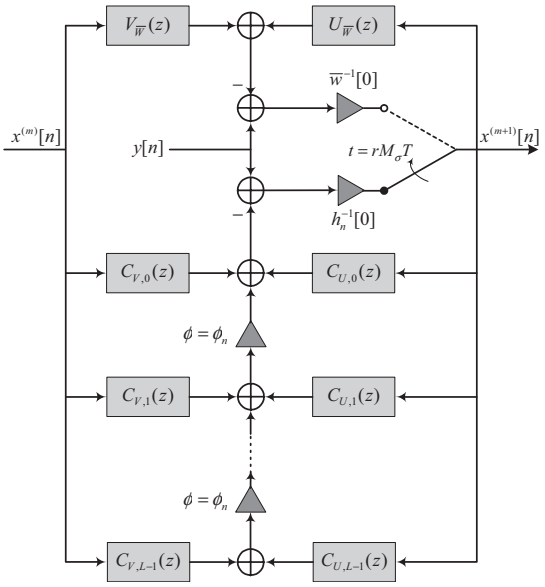

Fig. 5. VDF-based compensation structure in the mth GSI.

TABLE I

IMPLEMENTATION COMPLEXITIES OF THE GSI AND RI IN ONE ITERATION. VDF SUBFILTER LENGTH: $P_h = N_{h1} + N_{h2} + 1$ SUBFILTER NUMBER L HIGH-PASS FILTER LENGTH: $P_w = 2N_w + 1$

	$n \neq rM_\sigma$			$n = rM_\sigma$	
	Number of fixed filter coefficients	ϕ_n	$h^{-1}[0,\phi_n]$	Number of fixed filter coefficients	$w^{-1}[0]$
GSI	$(N_{h1}+N_{h2})L$	$L-1$	1	$2N_w$	1
RI	P_hL	$L-1$	N/A	P_wL	N/A

where $s_1^{(m)}[n]$ can be viewed as an output of filtering $x^{(m+1)}[n]$ by an M'-periodic time varying filter $U_n(z) = \sum_{n_0 \geq 1} \tilde{h}_n[n_0] z^{-n}$ and similarly $s_2^{(m)}[n]$ as an output of filtering $x^{(m)}[n]$ by $V_n(z) = \sum_{n_0 \leq 1} \tilde{h}_n[n_0] z^{-n}$. By the definition of (37), at time instant $n = rM_\sigma$, we have $U_n(z) = U_{\bar{W}}(z) = \sum_{n_0=1}^{N_w} \bar{w}_n[n_0] z^{-n}$ and $V_n(z) = V_{\bar{W}}(z) = \sum_{n_0=-1}^{-N_w} \bar{w}_n[n_0] z^{-n}$. At the other time instants, $U_n(z)$ and $V_n(z)$ can be realized using the VDF model in (9). More precisely, they are given by $V_n(z) = V(z, \phi_n) = \sum_{l=0}^{L-1} C_{V,l}(z) \phi_n^l$ and $U_n(z) = U(z, \phi_n) = \sum_{l=0}^{L-1} C_{U,l}(z) \phi_n^l$, where $C_{V,l}(z) = \sum_{n_0=-1}^{-N_h} c_l[n_0] z^{-n}$ and $C_{U,l}(z) = \sum_{n_0=1}^{N_h} c_l[n_0] z^{-n}$ are the lth subfilter of $U(z, \phi)$ and $V(z, \phi)$. Fig. 5 suggests a VDF-based structure for the implementation of GSI. In this structure, all the filter coefficients of $U_{\bar{W}}(z)$, $V_{\bar{W}}(z)$, $C_{V,l}(z)$, and $C_{U,l}(z)$ are fixed, and only a few variable multipliers are required for the tuning parameter ϕ. Similarly, the RI can be implemented using VDF, though the recursive structure is not required [14], [15]. The general implementation complexities of the GSI and RI are shown in the Table I. We can see that both iterative structures offer similar complexity. For the GSI particularly, we can also see that the time-dependent variable multipliers are solely required at $n \neq rM_\sigma$ for the multiplications with ϕ_n and $h^{-1}[0, \phi_n]$, while the remaining multiplications are all fixed. Although the fixed multipliers seem to contribute to the major portion of hardware cost, the same multiplier-less realization approaches mentioned in Section II can be

applied here to replace them with limited number of adders and shifters. Therefore, the proposed structure is computationally efficient in the sense that there are only a few expensive variable multipliers in one iteration. Moreover, it is shown in [53] that the convergence of the proposed algorithm is generally guaranteed with M_σ satisfying (23). In real applications, a reasonable input bandwidth efficiency related to ε in (1) always leads to an appropriate choice of M_σ which ensures that the problem is solvable and the proposed iterative framework is convergent. These useful properties, in addition to the superior convergence performance of the GSI, make the proposed iterative framework very suitable to high-speed and real-time applications.

Before proceeding, we would like to give several remarks to the proposed iterative framework.

1) Acceleration of the Proposed Iterative Framework: Motivated by the conventional iterative framework in (26) and (27), it is natural to consider the following iteration:

$$\boldsymbol{x}^{(m+1)} = \tilde{\boldsymbol{G}}\tilde{\boldsymbol{W}}\boldsymbol{x}^{(m)} + \tilde{\boldsymbol{B}}^{-1}\boldsymbol{y} \tag{39}$$

where

$$[\tilde{\boldsymbol{W}}]_n = \begin{cases} [\boldsymbol{W}]_n, & n = rM_\sigma \\ [\boldsymbol{I}]_n, & \text{otherwise.} \end{cases} \tag{40}$$

Comparing with (35), the low-pass filtering prior knowledge in (25) is utilized again to improve the approximation of $\boldsymbol{x}^{(m)}$ obtained in the previous iteration. In particular, we are only interested in time instants $n = rM_\sigma$ when the samples of $y[n]$ are purposely discarded for the foreground estimation. It is expected that the prior knowledge can help to further speed up the convergence. Since this slight modification is just a prefiltering of $\boldsymbol{x}^{(m)}$, it does not alter the efficient implementation structure mentioned earlier. The price to pay is an extra complexity of low-pass filtering at $n = rM_\sigma$ per iteration. The corresponding RI-based and GSI-based iterations will be called the accelerated RI-based (aRI) and accelerated GSI-based (aGSI) algorithms, respectively.

2) Alternate Missing Sample Pattern: As discussed in Section III, the time instants for the disposal of $y[n]$ are fixed at $n = rM_\sigma$ only because it results in a regular update structure which is suitable to high-speed and real-time TI ADC application. In fact, the proposed iterative framework is also applicable to other arbitrary missing sample pattern as long as (23) is satisfied. This is attributed to another major advantage of the proposed algorithm that the assumption of periodic time-varying nature of the system is indeed not required. Such nice property also suggests that the complexity of the proposed framework is independent of the number of channels and it is very effective in adapting to any possible system changes.

As an example of missing sample pattern, we may assume that the missing samples are contiguously distributed. In view of the proposed system, a possible way to achieve this setting is to discard the samples of all sub-ADCs at a time and wait for the next disposal so as to ensure (23) is satisfied. In this way, the regular estimation and compensation structure can still be kept. However, it should be noted the resulting missing sample problem reduces to so-called extrapolation problem, which could sometimes lead to ill-conditioned system of linear of equations as suggested in [40]. Very often, its main adverse effect is the degradation of the convergence performance of the iterative algorithms. On the other hand, the uniform missing sample pattern considered in this paper is usually more desirable in providing a better conditioned system and enhancing the convergence rate of the iterative algorithms. Also, it facilitates the development of regular estimation and compensation structures as we discussed earlier.

3) Application to Image Restoration and Other High-Dimension Problems: Most iterative algorithms for missing sample problem are mainly dedicated to the application of image restoration and super resolution [41]–[48]. By the same token, the proposed algorithm can also be generalized to solve similar higher dimensional problem as long as it can be formulated as a system of linear equations.

4) Extension to Handle Multiple Types of Frequency Response Mismatches: In [21], we have proposed an extended iterative structure which is able to cope with time-varying systems involving more than one type of frequency response mismatches such as timing and bandwidth mismatches. More precisely, the resulting structure can be realized as a cascade of iterative structures, each of which compensates for different types of mismatches. A similar idea can be applied to the proposed iterative structure, but details are omitted due to page limitations.

VI. Examples

A. Offset, Gain, and Timing Mismatches

In this example, we shall investigate the performance of the proposed estimation and iterative algorithms by means of computer simulations. As an illustration, we consider a four-channel TI ADC (i.e., $M = 4$) with offset mismatch $\alpha_k = [-0.03, 0.05, -0.08, -0.02]$, gain mismatch $\beta_k = [0.05, -0.04, 0.02, -0.09]$, and timing mismatch $\phi_k = [0.01, -0.05, 0.04, -0.03]$. We also assume that the input signal to be sampled is given by $x[n] = \sum_{i=1}^{10} \cos(n\omega_i)$, with $\omega_i = 2i\pi/25$, and hence its maximum frequency is 0.8π. This implies that the band-limiting parameter in (1) is given by $\varepsilon = 0.8$. Therefore, we can set $M_\sigma = 7$ from (11) and (23) to ensure that the estimation module has a regular update structure and the recovery of $x[n]$ is guaranteed in the compensation module.

Before proceeding to the performance evaluation, we briefly illustrate how to design an appropriate VDF for the timing mismatch model reported in [15] and [21]. The channel frequency response of the timing mismatch can be expressed as $F_n(j\Omega) = e^{-j\Omega T\phi_n}$ or, equivalently, in DT domain as

$$F_n(e^{j\omega}) = e^{-j\omega\phi_n} \tag{41}$$

where ϕ_n denotes the time offsets with respect to the ideal sampling time $t = nT$. We can see that the response $F_n(e^{j\omega})$ varies with a single spectral parameter ϕ_n, and therefore it can be expressed as a function of frequency ω and spectral parameter ϕ, i.e., $F(e^{j\omega}, \phi_n) = F_n(e^{j\omega})$. As discussed in Section IV, we employ a VDF $h[n_0, \phi]$ in the form of (9) to approximate $F(e^{j\omega}, \phi_n)$. For example, it can be designed

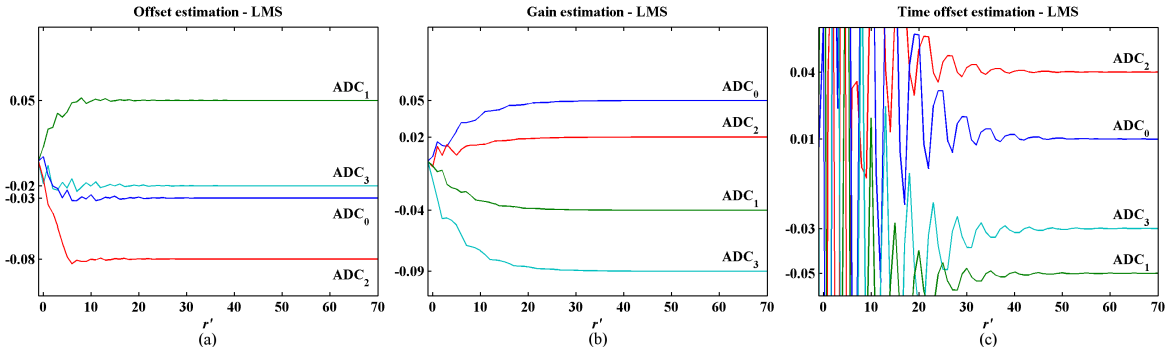

Fig. 6. Convergence of the LMS estimation algorithm for (a) offset α_k, (b) gain β_k, and (c) timing ϕ_k mismatches in a four-channel TIADC with $\alpha_k = [-0.03, 0.05, -0.08, -0.02]$, $\beta_k = [0.05, -0.04, 0.02, -0.09]$, and $\phi_k = [0.01, -0.05, 0.04, -0.03]$.

by solving the following minimax problem:

$$\min \max_{(\omega,\phi)\in\Psi} \left| H(e^{j\omega}, \phi) - F(e^{j\omega}, \phi) \right| \tag{42}$$

where Ψ collectively denotes the frequency and tuning range of interest, and $H(e^{j\omega}, \phi)$ is the frequency response of $h[n_0, \phi]$. Once it is solved, we obtain the VDF sub filter coefficients $c_l[n_0]$ in (9), which will be used in both estimation and iterative compensation modules. In principle, these modules can utilize different VDFs depending on the required accuracy and complexity.

1) Evaluation of Estimation Module: In the estimation module, we further assume that the known input signal $\sigma(t)$ is a single sinusoidal signal with frequency $0.8\pi/M'$. For the timing mismatch estimation, special care has to be taken on the actual value of the estimate $\hat{\phi}_k$ that will be passed to the compensation module. To be specific, consider the sampling interval of $\sigma_k[r'] = \sigma_c(r'M'T + rM_\sigma T - \phi_k T)$, where $k = \text{mod}(rM_\sigma, M)$, as defined in Section III. When comparing with the original sampling instant at $t = nT - \phi_n T = nT - \phi_k T$, $k = n \bmod M$, one can notice that the estimation module will indeed return an estimate of ϕ_k/M' (instead of ϕ_k) because the rate of $\sigma_k[r']$ is M' times slower. Hence, the actual estimate passed to the compensation module should be $M'\hat{\phi}_k$. According to the maximum frequency of $\sigma(t)$, the rate of $\sigma_k[r']$ and the maximum tuning range of ϕ_k discussed earlier, Ψ of the VDF in (42) can be chosen as $\omega \in [-0.8\pi, 0.8\pi]$ and $\phi \in [-0.05/M', 0.05/M']$. For illustration purposes, we shall employ a VDF with $N_{h1} = N_{h2} = N_h = 15$ and $L = 3$ subfilters, which is designed using the method in [50]. Figs. 6 and 7 show the estimates of various mismatches obtained, respectively, using the LMS algorithm with an adaption step size $\mu = 0.2$ and the NLMS algorithm with $\mu = 1$ and $\zeta = 1 \times 10^{-6}$. We can see that all the estimates of mismatches agree very well with the true ones for both algorithms, and the NLMS algorithm appears to converge faster than the LMS algorithm. Although the LMS algorithm takes a longer time to reach the desired values, its step size can be set larger to enhance the convergence rate. However, as a fundamental tradeoff, its excess mean square error also increases with the step size [39], which could in turn degrade the overall system performance. The NLMS algorithm has similar property, but it is relatively less sensitive to the choice of μ because of the additional normalization term $\left\|\nabla e[r', \hat{\gamma}_k[r']\right\|^2$ in (22). Owing to this, the NLMS algorithm is a better option for its simpler parameter selection in practical implementation although it has a slightly higher complexity.

2) Evaluation of Compensation Module: Now we evaluate the performance of the proposed iterative framework in (35) and its accelerated version in (39) as mentioned in Section V-C. In particular, the GSI, aGSI, RI, and aRI are considered. In order to fully assess their ultimate capability, we assume that all the mismatches have already been precisely estimated. As a comparison, we also consider the CIA in (26), RIA in (29), and biconjugate gradient-stabilized method (BiCGSTAB) in [51]. The latter is considered here because it is arguably one of the fastest iterative algorithms in the literature for solving nonsymmetric linear systems, and therefore can be used as a benchmark to illustrate how fast an iterative algorithm can perform. However, despite its expected superior convergence performance, we note that, as a block-based algorithm, it is indeed not suitable to real-time TI ADC application because its complexity, in general, increases exponentially with the unknown number of samples N. In the comparison, the BiCGSTAB algorithm is used to solve the nonsymmetric linear system in (33) which is identical to that solved by the proposed iterative framework. To establish the linear system in (33), we first design the VDF with the following specifications: $N_{h1} = N_{h2} = N_h = 25$, $L = 4$, $\omega \in [-0.8\pi, 0.8\pi]$, and $\phi \in [-0.05, 0.05]$. Then, we design the low-pass filter $w[n_0]$ with $2N_w = 132$, pass-band cutoff frequency of 0.8π, and stop-band cutoff frequency of 0.9π, and obtain the required high-pass filter $\bar{w}[n_0]$ as defined in (30). All the algorithms are assessed using the signal-to-noise-and-distortion ratio (SNDR) as follows:

$$\text{SNDR}_a^{(m)} = \sum\nolimits_{n=0}^{N-1} |x[n]|^2 \Big/ \sum\nolimits_{n=0}^{N-1} \left| x[n] - x^{(m)}[n] \right|^2. \tag{43}$$

Fig. 8 shows the convergence performances of various algorithms in terms of the SNDR. In particular, we can see from Fig. 8(a) that the BiCGSTAB, aGSI, and GSI converge within 10 iterations and they significantly outperform the aRI, RI, CIA, and RIA. Among the least four algorithms, the RIA exhibits the lowest convergence rate, but we note that an optimal regularization parameter λ in (29) may have a

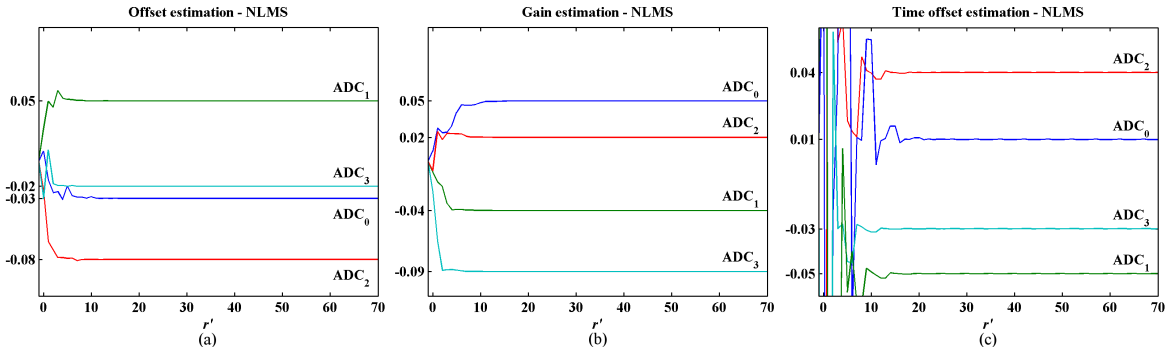

Fig. 7. Convergence of the NLMS estimation algorithm for (a) offset α_k, (b) gain β_k, and (c) timing ϕ_k mismatches in a four-cbannel TIADC with $\alpha_k = [-0.03, 0.05, -0.08, -0.02]$, $\beta_k = [0.05, -0.04, 0.02, -0.09]$, and $\phi_k = [0.01, -0.05, 0.04, -0.03]$.

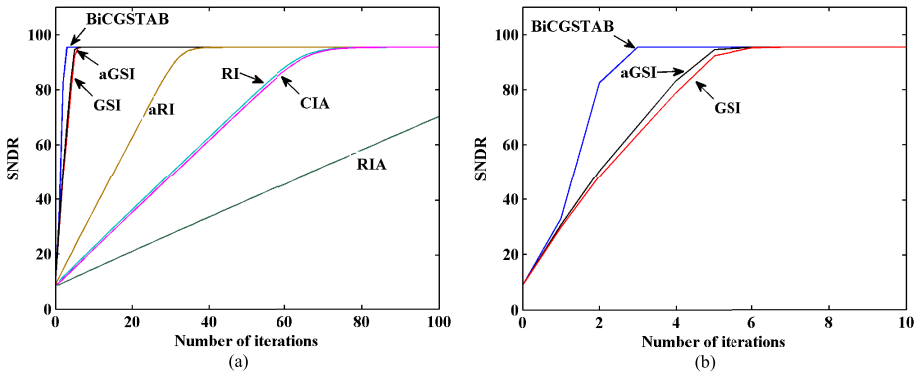

Fig. 8. SNDR performances of various iterative algorithms in (a) 100 iterations and (b) 10 iterations particularly for the easier discrimination between BiCGSTAB, a GSI, and GSI.

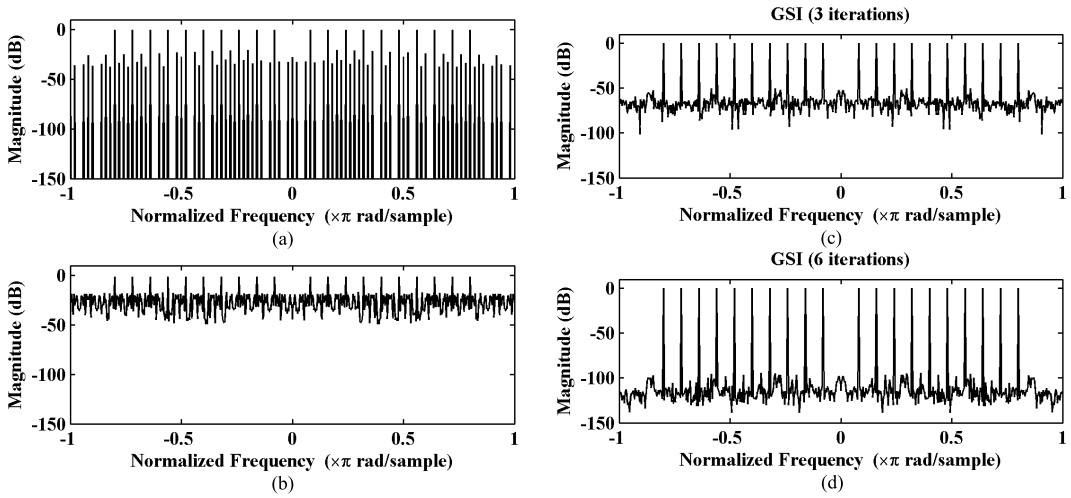

Fig. 9. (a) Uncompensated output spectrum of $y[n]$. (b) Uncompensated output spectrum of $\tilde{y}[n]$. Output spectra obtained using the GSI after (c) three and (d) six iterations.

positive impact on the convergence rate [48]. Unfortunately, finding such optimal value is nontrivial, and in this example we only choose it as $\lambda = 0.9$ in a trial-and-error manner, which seems to be the best value in a number of trials. Moreover, while the RI and CIA offer similar performance, the simple acceleration scheme introduced in Section V further improves the convergence rate of the RI from about 70 to 30 iterations. On the other hand, having a closer look at the three faster iterative algorithms shown in Fig. 8(b), we can see that the BiCGSTAB, aGSI, and GSI actually converge to about 95 dB SNDR in three, five, and six iterations, respectively. Although the GSI is slightly inferior to the BiCGSTAB, its efficient filtering structure discussed in Section V-C makes it more attractive than the block-based BiCGSTAB especially in real-time TI ADC application. To further illustrate the performance of the proposed iterative compensation framework, we show in Fig. 9 the spectra of the uncalibrated signal $y[n]$, the zero-inserted uncalibrated signal $\tilde{y}[n]$, and the corrected signals after three and six iterations of the GSI. Their maximum undesired tones are, respectively, found to be –20.49, –16.89, –50.28, and –94.31 dB. Such improvement (73.82 dB for $y[n]$ and 77.42 dB for $\tilde{y}[n]$) illustrates the usefulness of

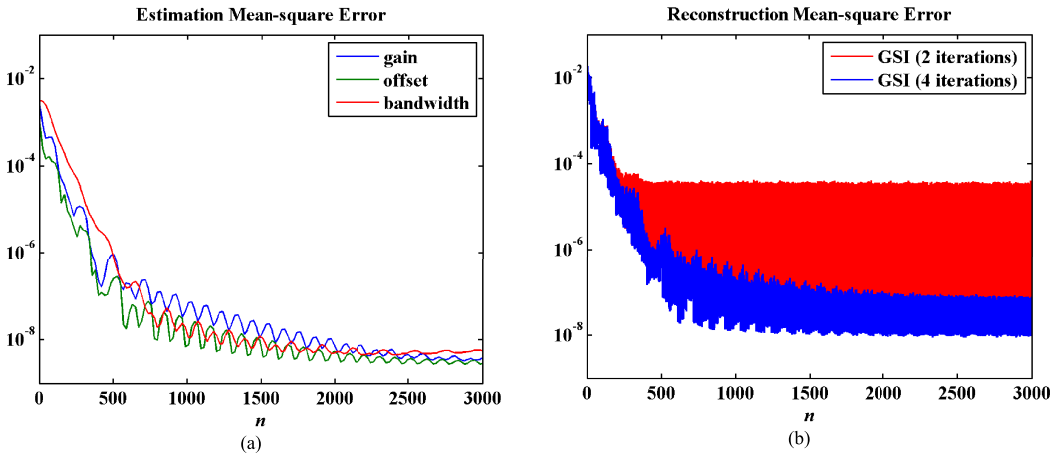

Fig. 10. Mean-square error convergence behavior of the (a) estimation and (b) compensation modules evolved in time for a Monte Carlo simulation with 1000 trials.

the proposed iterative framework in compensating for the frequency response mismatch even under the situation of partly missing samples. In [53], we have also demonstrated the multiplierless realization of the proposed iterative structure and the effect of signal round-off error on the maximum achievable SNDR. Unfortunately, details are omitted due to page limitation. Interested readers are referred to [53] for more details.

B. Offset, Gain, and Bandwidth Mismatches

Unlike the settings of the previous example, we shall now evaluate the performance of the proposed calibration algorithm when it is operated in tandem with the estimation and compensation modules. Moreover, we shall consider a practical scenario where the overall system suffers from both quantization and estimation errors. To illustrate the versatility of the proposed approach, we consider another type of frequency response mismatch, called bandwidth mismatch in [17], [20], and [21], which is defined as follows:

$$F_n(j\Omega) = \frac{1}{1+j\frac{\Omega}{\Omega_n^c}} \frac{1-e^{-(\Omega_n^c T + j\Omega T)}}{1-e^{-(\Omega_n^c T + jM\Omega T)}} \tag{44}$$

where Ω_n^c is a time-varying cutoff frequency. Similar to the timing mismatch model, the equivalent DT representation of (44) in terms of a single spectral parameter ϕ_n can be expressed as

$$F_n(e^{j\omega}) = F(e^{j\omega}, \phi_n) = \frac{1}{1+j\frac{\omega}{(1+\phi_n)\pi}} \frac{1-e^{-[(1+\phi_n)\pi + j\omega]}}{1-e^{-[(1+\phi_n)\pi + jM\omega]}} \tag{45}$$

where $\phi_n = \Omega_n^c T/\pi - 1$. However, as suggested in [21], directly deconvoluting with the time-varying filter $h_n(n_0)$ that approximates $F_n(e^{j\omega})$ in (3) is not recommended because the associated system matrix $\boldsymbol{A}$ in (4) is in general not a diagonal dominant matrix. In this specific case, more number of iterations is usually required. To avoid this problem, we follow the approach in [21] and approximate the ideal response, say, $F(e^{j\omega}, \phi)/F(e^{j\omega}, 0)$[instead of $F(e^{j\omega}, \phi)$] by the VDF $H(e^{j\omega}, \phi)$. By so doing, the system matrix $\boldsymbol{A}$ becomes more diagonally dominanant and exhibits better condition number. Consequently, the convergence rate of the iterative framework in (5) for solving (4) will be improved. Since the proposed iterative framework is also developed based on (4), its convergence rate would similarly be benefited from the better conditioned system matrix. We note, however, that the recovered spectrum would be $F(e^{j\omega}, 0)X(e^{j\omega})$ instead of the target spectrum $X(e^{j\omega})$, and hence an additional equalization module is required to compensate for $F(e^{j\omega}, 0)$ after iterative compensation of frequency response mismatches. Since $F(e^{j\omega}, 0)$ is time-invariant and predetermined, equalizing it is preferable to the growth of the complexity due to the increased number of iterations.

To study the average behavior of the proposed estimation and compensation algorithms, a Monte Carlo (MC) simulation with $P = 1000$ trials is carried out. The system configuration and filter parameters that will be considered in this example are summarized as follows: 1) the number of channels is $M = 3$ and the resolution of the sub-ADCs is 12 bits; 2) the offset α_k, gain β_k, and bandwidth mismatch parameter ϕ_k in (12) are randomly chosen in the interval $[-0.1, 0.1]$ for $k = 0, 1, 2$; 3) the target input is a white Gaussian signal band-limited to 0.8π, starting from $n = 0$ to $n = 3000$; 4) the missing sampling factor is $M_\sigma = 7$ and the known input $\sigma(t)$ is a sinusoidal signal with single frequency $0.8\pi/M'$; 5) the NLMS algorithm is employed in the estimation module with $\mu = 1$ and $\zeta = 1 \times 10^{-6}$; 6) the parameters of VDF $H(e^{j\omega}, \phi)$ for both estimation and iterative compensation modules are $\omega \in [-0.8\pi, 0.8\pi]$, $\phi \in [-0.1, 0.1]$, $N_h = 20$ and $L = 4$; and 7) the pass-band cutoff frequency, stop-band cutoff frequency, and filter length of the low-pass filter $W(e^{j\omega})$ are, respectively, 0.8π, 0.9π, and 103.

According to Section III, the estimated mismatch vector $\hat{\boldsymbol{\gamma}}_k[r']$ of the kth sub-ADC is updated at $n = r'M' + rM_\sigma$ with $k = \text{mod}(rM_\sigma, M)$. Thus, in order to investigate how the performance of the estimation module evolves with increasing sampling instant n, we consider the following mean-square error (MSE):

$$e_{\text{EST}}[r'M'] = \frac{1}{P}\sum_{i=1}^{P}\frac{1}{M}\sum_{k=0}^{M-1}\left|\hat{\gamma}_k^{(i)}[r'] - \gamma_k[r']\right|^2 \tag{46}$$

where γ_k denotes either α_k, β_k or ϕ_k, and the superscript (i) denotes the ith trial of the MC simulation. We can see from Fig. 10(a) that $e_{\mathrm{EST}}[r'M']$ quickly converges to the level of 1×10^{-7} in less than $1000T$, and eventually settles at the level of 1×10^{-8}, which is mainly due to the error floor caused by the quantization noise.

On the other hand, the performance of the proposed iterative compensation algorithm is assessed using

$$e_x^{(m)}[n] = \frac{1}{P} \sum_{i=1}^{P} \left| x^{(m),(i)}[n] - x[n] \right|^2 \tag{47}$$

where $x^{(m),(i)}[n]$ denotes the solution obtained in the ith trial after m iterations. As an illustration, we only consider the GSI with two and four iterations, as shown in Fig. 10(b). We can see that $e_x^{(4)}[n]$ converges to a much deeper level than $e_x^{(2)}[n]$, as expected. Moreover, $e_x^{(4)}[n]$ basically follows the convergence curve of $e_{\mathrm{EST}}[r'M']$, which demonstrates that the iterative compensation structure responses almost instantaneously with an improving estimate of mismatch parameters as n increases, thanks to the efficient filtering structure. To further quantify its performance, we consider the average SNDR over P trials, and for each trial we compute the SNDR in (43) from $n = 1000$ to $n = 3000$ samples. The average SNDR of the corrected signal obtained after two and four iterations of GSI are, respectively, found to be 51.56 and 72.17 dB. For the latter, this implies an improvement of 50.61 dB for the uncalibrated signal $y[n]$ and 63.7 dB for the zero-inserted uncalibrated signal $\tilde{y}[n]$. Also, we note that an average SNDR of 72.17 dB is already very close to the theoretical SNDR estimated from the 12-bit resolution of the sub-ADCs. In this case, increasing the number of iterations to more than four will not further improve the performance, as the noise floor is mainly dominated by the quantization error. For example, if 10-bit sub-ADCs are used instead, the noise floor in Fig. 10(b) rises to an error level of about 1×10^{-6} because of the larger quantization error. However, the simulation results are omitted because of page limitations. The above results demonstrate that the proposed calibration approach is able to achieve satisfactory reconstruction accuracy in less than 1000 samples. In fact, such convergence performance is far better than that of other conventional blind calibration approaches, which usually converge in more than 10^4–10^6 samples. Moreover, the NLMS algorithm also allows slow time-varying mismatches to be tracked online.

VII. Conclusion

An efficient online calibration structure to estimate and compensate for mismatches in M-channel TI ADCs was presented. To illustrate the versatility of the proposed approach, we investigated the simultaneous calibration of offset, gain, and frequency response mismatches that are mostly considered in the literature. The overall calibration structure was formed by a combination of novel estimation and iterative compensation modules, both of which are applicable to arbitrary number of channels and can be efficiently implemented using VDF. The former is able to estimate and track the possibly changing channel mismatches accurately, whereas the latter is useful in online compensation of these mismatches with low complexity. Through computer simulations, we have shown that the estimation and iterative compensation modules are individually very effective in achieving satisfactory performance with small number of iterations. When these modules work in tandem for the calibration purpose, simulation results also demonstrate the superior performance of the proposed calibration structure in terms of the convergence time and reconstruction accuracy.

A possible extension of the work is to study the stability of the proposed iterative compensation structure due to the time-varying and recursive natures of the GSI-based structure. Another commonly considered problem is the signal round-off analysis [52], which is particularly important to the determination of bit accuracy at the TI ADC's output. Because of page limitations, these issues will be reported in a future work.

References

[1] S. C. Chan, K. M. Tsui, K. S. Yeung, and T. I. Yuk, "Design and complexity optimization of a new digital IF for software radio receivers with prescribed output accuracy," *IEEE Trans. Circuits Syst. I, Reg. Papers*, vol. 54, no. 2, pp. 351–366, Feb. 2007.

[2] P. Ferrari, A. Flammini, and E. Sisinni, "New architecture for a wireless smart sensor based on a software-defined radio," *IEEE Trans. Instrum. Meas.*, vol. 60, no. 6, pp. 2133–2141, Jun. 2011.

[3] W. C. Black and D. A. Hodges, "Time interleaved converter arrays," *IEEE J. Solid-State Circuits*, vol. 15, no. 6, pp. 1022–1029, Dec. 1980.

[4] A. Petraglia and S. K. Mitra, "Analysis of mismatch effects among A/D converters in a time-interleaved waveform digitizer," *IEEE Trans. Instrum. Meas.*, vol. 40, no. 5, pp. 831–835, Oct. 1991.

[5] C. Vogel, "The impact of combined channel mismatch effects in time-interleaved ADCs," *IEEE Trans. Instrum. Meas.*, vol. 54, no. 1, pp. 415–427, Feb. 2005.

[6] Y. C. Jenq, "Perfect reconstruction of digital spectrum from nonuniformly sampled signals," *IEEE Trans. Instrum. Meas.*, vol. 46, no. 3, pp. 649–652, Jun. 1997.

[7] Y. C. Eldar and A. V. Oppenheim, "Filterbank reconstruction of bandlimited signals from nonuniform and generalized samples," *IEEE Trans. Signal Process.*, vol. 48, no. 10, pp. 2864–2875, Oct. 2000.

[8] R. S. Prendergast, B. C. Levy, and P. J. Hurst, "Reconstruction of bandlimited periodic nonuniformly sampled signals through multirate filter banks," *IEEE Trans. Circuits Syst. I, Reg. Papers*, vol. 51, no. 8, pp. 1612–1622, Aug. 2004.

[9] H. Johansson and P. Löwenborg, "Reconstruction of nonuniformly sampled bandlimited signals by means of time-varying discrete-time FIR filters," *EURASIP J. Appl. Signal Process.*, pp. 1–18, Jan. 2006.

[10] J. Selva, "Functionally weighted Lagrange interpolation of band-limited signals from nonuniform samples," *IEEE Trans. Signal Process.*, vol. 57, no. 1, pp. 168–181, Jan. 2009.

[11] S. Tertinek and C. Vogel, "Reconstruction of nonuniformly sampled bandlimited signals using a differentiator–multiplier cascade," *IEEE Trans. Circuits Syst. I, Reg. Papers*, vol. 55, no. 8, pp. 2273–2286, Sep. 2008.

[12] Y. C. Lim, Y. X. Zou, J. W. Lee, and S. C. Chan, "Time-interleaved analog-to-digital-converter compensation using multichannel filters," *IEEE Trans. Circuits Syst. I, Reg. Papers*, vol. 56, no. 10, pp. 2234–2347, Oct. 2009.

[13] Y. X. Zou, S. L. Zhang, Y. C. Lim, and X. Chen, "Timing mismatch compensation in time-interleaved ADCs based on multichannel Lagrange polynomial interpolation," *IEEE Trans. Instrum. Meas.*, vol. 60, no. 4, pp. 1123–1131, Apr. 2011.

[14] K. M. Tsui, "Efficient design and realization of digital IFs and time-interleaved analog-to-digital converters for software radio receivers," Ph.D. dissertation, Dept. Electr. Electron. Eng., Univ. Hong Kong, Hong Kong, Jul. 2008.

[15] K. M. Tsui and S. C. Chan, "A versatile iterative framework for the reconstruction of bandlimited signals from their nonuniform samples," *J. Signal Process. Syst.*, vol. 62, no. 3, pp. 459–468, Mar. 2010.

[16] M. Seo, M. Rodwell, and U. Madhow, "Comprehensive digital correction of mismatch errors for a 400-Msamples/s 80-dB SFDR time-interleaved analog-to-digital converter," *IEEE Trans. Microw. Theory Tech.*, vol. 53, no. 3, pp. 1072–1082, Apr. 2005.

[17] T. H. Tsai, P. J. Hurst, and S. H. Lewis, "Bandwidth mismatch and its correction in time-interleaved analog-to-digital converters," *IEEE Trans. Circuits Syst. II, Exp. Briefs*, vol. 53, no. 10, pp. 1133–1137, Oct. 2006.

[18] H. Johansson and P. Löwenborg, "A least-squares filter design technique for the compensation of frequency-response mismatch errors in time interleaved A/D converters," *IEEE Trans. Circuits Syst. II, Exp. Briefs*, vol. 55, no. 11, pp. 1154–1158, Nov. 2008.

[19] H. Johansson, "A polynomial-based time-varying filter structure for the compensation of frequency-response mismatch errors in time-interleaved ADCs," *IEEE J. Sel. Topics Signal Process.*, vol. 3, no. 3, pp. 384–396, Jun. 2009.

[20] C. Vogel and S. Mendel, "A flexible and scalable structure to compensate frequency response mismatches in time-interleaved ADCs," *IEEE Trans. Circuits Syst. I, Reg. Papers*, vol. 56, no. 11, pp. 2463–2475, Nov. 2009.

[21] K. M. Tsui and S. C. Chan, "New iterative framework for frequency response mismatches correction in time-interleaved ADCs: Design and performance analysis," *IEEE Trans. Instrum. Meas.*, vol. 60, no. 12, pp. 3792–3805, Dec. 2011.

[22] Y. C. Jenq, "Digital spectra of nonuniformly sampled signals: A robust sampling time offset estimation algorithm for ultra high-speed waveform digitizer using interleaving," *IEEE Trans. Instrum. Meas.*, vol. 39, no. 1, pp. 71–75, Jun. 1990.

[23] H. Jin and E. K. F. Lee, "A digital-background calibration technique for minimizing timing-error effects in time-interleaved ADCs," *IEEE Trans. Circuits Syst. II, Analog Digit. Signal Process.*, vol. 47, no. 7, pp. 603–613, Jul. 2000.

[24] T. Strohmer and J. Xu, "Fast algorithms for blind calibration in time interleaved analog-to-digital converters," in *Proc. IEEE ICASSP*, Apr. 2007, pp. 1225–1228.

[25] V. Divi and G. Wornell, "Blind calibration of timing skew in time-interleaved analog-to-digital converters," *IEEE J. Sel. Topics Signal Process.*, vol. 3, no. 3, pp. 509–522, Jun. 2009.

[26] D. Fu, K. C. Dyer, S. H. Lewis, and P. J. Hurst, "A digital background calibration technique for time-interleaved analog-to-digital converters," *IEEE J. Solid-State Circuits*, vol. 33, no. 12, pp. 1904–1911, Dec. 1998.

[27] P. Satarzadeh, B. C. Levy, and P. J. Hurst, "A parametric polyphase domain approach to blind calibration of timing mismatches for M-channel time-interleaved ADCs," in *Proc. IEEE ISCAS*, May 2010, pp. 4053–4056.

[28] Z.-L. Li, B. Yan, and W.-J. Shi, "Adaptive blind calibration of timing mismatches for time-interleaved ADCs based on differentiator multiplier cascade," in *Proc. IEEE ICCP*, Oct. 2011, pp. 308–311.

[29] S. Huang and B. C. Levy, "Blind calibration of timing offset for four-channel time-interleaved ADCs," *IEEE Trans. Circuits Syst. I, Reg. Papers*, vol. 54, no. 4, pp. 863–876, Apr. 2006.

[30] M. Seo and M. Rockwell, "Generalized blind mismatch correction for a two-channel time-interleaved ADC: Analytic approach," in *Proc. IEEE ISCAS*, May 2007, pp. 109–112.

[31] P. Satarzadeh, B. C. Levy, and P. J. Hurst, "Adaptive semiblind calibration of bandwidth mismatch for two-channel time-interleaved ADCs," *IEEE Trans. Circuits Syst. I, Reg. Papers*, vol. 56, no. 9, pp. 2075–2088, Sep. 2009.

[32] M. Jridi, "A subband FFT-based method for static errors compensation in time-interleaved ADCs," in *Proc. IEEE MWSCAS*, Aug. 2011, pp. 1–4.

[33] S. Huang and B. C. Levy, "Adaptive blind calibration of timing offset and gain mismatch for two-channel time-interleaved ADCs," *IEEE Trans. Circuits Syst. I, Reg. Papers*, vol. 53, no. 6, pp. 1278–1288, Jun. 2006.

[34] C. Vogel, S. Saleem, and S. Mendel, "Adaptive blind compensation of gain and timing mismatches in M-channel time-interleaved ADCs," in *Proc. IEEE ICECS*, Sep. 2008, pp. 49–52.

[35] S. Saleem and C. Vogel, "Adaptive blind background calibration of polynomial-represented frequency response mismatches in a two-channel time-interleaved ADC," *IEEE Trans. Circuits Syst. I, Reg. Papers*, vol. 58, no. 6, pp. 1300–1310, Jun. 2011.

[36] C. W. Farrow, "A continuously variable digital delay element," in *Proc. IEEE ISCAS*, vol. 3. Jun. 1988, pp. 2641–2645.

[37] C. K. S. Pun, S. C. Chan, K. S. Yeung, and K. L. Ho, "On the design and implementation of FIR and IIR digital filters with variable frequency characteristics," *IEEE Trans. Circuits Syst. II, Analog Digit. Signal Process.*, vol. 49, no. 11, pp. 689–703, Nov. 2002.

[38] A. G. Dempster and M. D. MacLeod, "Use of minimum-adder multiplier blocks in FIR digital filters," *IEEE Trans. Circuits Syst. II, Analog Digit. Signal Process.*, vol. 42, no. 9, pp. 569–577, Sep. 1995.

[39] A. H. Sayed, *Fundamentals of Adaptive Filtering*. New York, NY, USA: Wiley, 2003.

[40] F. Marvasti, *Nonuniform Sampling, Theory and Practice*. Norwell, MA, USA: Kluwer, 2001.

[41] R. W. Gerchberg, "Super resolution through error energy reduction," *Opt. Acta, Int. J. Opt.*, vol. 21, no. 9, pp. 709–720, 1974.

[42] A. Papoulis, "A new algorithm in spectral analysis and band-limited extrapolation," *IEEE Trans. Circuits, Syst.*, vol. 22, no. 9, pp. 735–742, Sep. 1975.

[43] P. J. S. G. Ferreira, "Interpolation and the discrete Papoulis-Gerchberg algorithm," *IEEE Trans. Signal Process.*, vol. 42, no. 10, pp. 2596–2606, Oct. 1994.

[44] P. J. S. G. Ferreira, "Noniterative and faster iterative methods for interpolation and extrapolation," *IEEE Trans. Signal Process.*, vol. 42, no. 11, pp. 3278–3282, Oct. 1994.

[45] D. C. Youla, "Generalized image restoration by the method of alternating orthogonal projections," *IEEE Trans. Circuits Syst.*, vol. 25, no. 9, pp. 694–702, Sep. 1978.

[46] R. W. Schafer, R. M. Mersereau, and M. A. Richards, "Constrained iterative restoration algorithms," *Proc. IEEE*, vol. 69, no. 4, pp. 432–450, Apr. 1981.

[47] A. K. Katsaggelos, J. Biemond, R. W. Schafer, and R. M. Mersereau, "A regularized iterative image restoration algorithm," *IEEE Trans. Signal Process.*, vol. 39, no. 4, pp. 914–929, Oct. 1991.

[48] M. G. Gang and A. K. Katsaggelos, "General choice of the regularization functional in regularized image restoration," *IEEE Trans. Image Process.*, vol. 4, no. 5, pp. 594–602, May 1995.

[49] J. S. Prater and C. M. Loeffler, "Analysis and design of periodically time-varying IIR filters, with applications to transmultiplexing," *IEEE Trans. Signal Process.*, vol. 40, no. 11, pp. 2715–2725, Nov. 1992.

[50] K. M. Tsui, S. C. Chan, and K. W. Tse, "Design of complex-valued variable digital filters and its application to the realization of arbitrary sampling rate conversions for complex signals," *IEEE Trans. Circuits Syst. II, Reg. Papers*, vol. 52, no. 7, pp. 424–428, Jul. 2005.

[51] H. Van der Vorst, "Bi-CGSTAB: A fast and smoothly converging variant of Bi-CG for the solution of nonsymmetric linear systems," *SIAM J. Sci. Stat. Comput.*, vol. 13, no. 2, pp. 631–644, Mar. 1992.

[52] S. C. Chan and K. M. Tsui, "Wordlength optimization of linear time invariant systems with multiple outputs using geometric programming," *IEEE Trans. Circuits Syst. I, Reg. Papers*, vol. 54, no. 4, pp. 845–854, Apr. 2007.

[53] K. M. Tsui and S. C. Chan, "Supplementary document: A novel iterative structure for online calibration of M-channel time-interleaved ADCs," Digit. Signal Process. Lab., Dept. EEE, Univ. Hong Kong, Hong Kong, Internal Rep. [Online]. Available: www.eee.hku.hk/∼kmtsui/TIM2013_supp_document.pdf

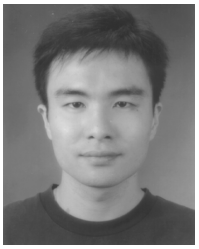

K. M. Tsui received the B.Eng., M.Phil., and Ph.D. degrees in electrical and electronic engineering from the University of Hong Kong, Hong Kong, in 2001, 2004, and 2008, respectively.

He is currently a Post-Doctoral Fellow with the Department of Electrical and Electronic Engineering, University of Hong Kong. His current research interests include high-speed AD converter architecture, array signal processing, biomedical signal processing, digital signal processing, multirate filter bank and wavelet design, and digital filter design, realization and application.

S. C. Chan (S'87–M'92) received the B.Sc.(Eng.) and Ph.D. degrees from the University of Hong Kong, Hong Kong, in 1986 and 1992, respectively.

He has been with the Department of Electrical and Electronic Engineering, University of Hong Kong, since 1994, where he is currently a Professor. His current research interests include fast transform algorithms, filter design and realization, multirate and biomedical signal processing, communications and array signal processing, high-speed A/D converter architecture, bioinformatics, and smart grid image-based rendering.

Dr. Chan is currently a member of the Digital Signal Processing Technical Committee of the IEEE Circuits and Systems Society. He is an Associate Editor of the IEEE TRANSACTIONS ON CIRCUITS AND SYSTEMS II and the *Journal of Signal Processing Systems and Digital Signal Processing*. He was the Chair of the IEEE Hong Kong Chapter of Signal Processing from 2000 to 2002, an Organizing Committee Member of the 2003 IEEE International Conference on Acoustics, Speech, and Signal Processing, the 2010 International Conference on Image Processing, and an Associate Editor of IEEE TRANSACTIONS ON CIRCUITS AND SYSTEMS I from 2008 to 2009.